Journal of Materials Chemistry C

Accepted Manuscript

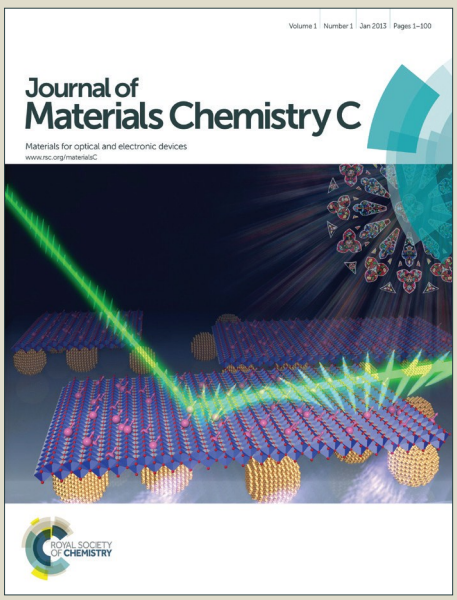

ROYAL SOCIETY OF CHEMISTRY

www.rsc.org/materialsC

Light-triggered Generation of Multifunctional Gas-Filled Capsules On-demand

Lei Wang[a,b,#], Jianying Wang[b,c,#], Kai Song[d,*], Weilong Li[b], Zhiqi Huang[b], Jintao Zhu[c], Xiaojun Han[a,*], and Zhihong Nie[b,*]

[a]State Key Laboratory of Urban Water Resource and Environment, School of Chemical Engineering and Technology, Harbin Institute of Technology, Harbin 150001, China

[b]Department of Chemistry and Biochemistry, University of Maryland, College Park, Maryland 20742, United States

[c]School of Chemistry and Chemical Engineering, Huazhong University of Science and Technology, Wuhan 430074, China

[d]School of Life science, Changchun Normal University, Changchun 130031, China

*E-mails: singsongderen@gmail.com; hanxiaojun@hit.edu.cn; znie@umd.edu

[#] These authors contributed equally to this work.

ABSTRACT: A combination of microfluidic technique and laser-triggered reaction has been developed to fabricate functional gas-filled capsules (GFCs) on-demand with applications such as a pressure sensor. This method involves: i) the generation of monodispersed alginate microcapsules containing ammonium bicarbonate (AB) as gas resource and gold nanorods as heating resource, in a microfluidic device; and ii) the near-infrared light-triggered generation of gases from the AB-containing microcapsules and simultaneous encapsulation of the gases in alginate shell to produce GFCs. Various functional substances such as dyes, quantum dots, and magnetic nanoparticles can be introduced into the shell of the GFCs to impart the system with multifunctionality. We further demonstrated the use of the GFCs as pressure sensors capable of sensing the variation in the pressure of environment.

Keywords: Gas-filled capsules (GFCs); alginate; ammonium bicarbonate; gold nanorods; pressure sensor.

INTRODUCTION

Gas bubbles are inherently unstable, as a result of the continuous dissolution of gas in surrounding liquid media.[1] Coating gas bubbles with a protective shell of polymers or biomolecules can effectively improve the stability of bubbles.[2-6] These gas-filled capsules (GFCs) show diverse applications in such as ultrasound imaging, drug delivery, and sensors.[7-14] Various methods for the fabrication of GFCs have been developed, including sonication[15, 16], high shear emulsification[17], inject printing[18] and droplet microfluidics[19-22]. In these approaches, GFCs are often generated and stored for future applications. However, encapsulated gas tends to escape from the GFCs because of the Laplace pressure across the air-water interface.[23-25] The stability of GFCs is strongly dependent on the property of protective materials. For instance, while bubbles coated with denatured albumin can be stored for up to years,[26] lipids stabilized gas bubbles can only be stored for less than one week.[27] The long-term instability of GFCs severely limits their potential applications. One promising strategy to solve the problem is to generate GFCs in a controlled manner immediately before their usage. Ammonium bicarbonate (AB) is usually used as a source of CO_2 gas in the food industry, as it decomposes into ammonia, carbon dioxide and water vapor in an endothermic process from 36 to 60 °C.[28, 29] We, therefore, hypothesize that the gases stored as a form of AB can be used to generate GFCs on-demand.

Herein, we developed a facile and robust approach to fabricate multifunctional GFCs with tunable size on-demand by combining microfluidic droplet generation and photothermal heating-triggered reaction. This method involves two steps: i) the microfluidic generation of monodispersed alginate microcapsules containing AB as gas resource and gold nanorods (AuNRs) which can convert light to heat; and ii) the near-infrared (NIR) light-triggered generation of gases from the AB-containing microcapsules and simultaneous encapsulation of the gases in alginate shell to produce GFCs. The GFCs generated are relatively uniform, and the size of GFCs can be readily tuned by controlling the initial droplet size and the concentration of calcium ions. Moreover, various functional substances such as fluorescence dyes, quantum dots (QDs), and magnetic nanoparticles (NPs) can be introduced into the shell of the GFCs to impart the system with multifunctionality. Finally, we further demonstrated that GFCs can be used as miniaturized pressure sensors for sensing pressure.

EXPERIMENTAL SECTION

Materials: $AgNO_3$, CTAB, sodium oleate, HCl, ascorbic acid, $HAuCl_4$, $NaBH_4$, $(NH_4)HCO_3$, CaI_2, alginate. $NH_3{\cdot}H_2O$, $FeCl_2{\cdot}4H_2O$, $FeCl_3{\cdot}6H_2O$, CdSe/ZnS, poly(vinyl alcohol) (PVA, Mw=13,000~23,000, 87-89% hydrolyzed) and fluorescein were all purchased from Sigma-Aldrich US and utilized as received. All the aqueous solution was prepared using ultrapure water.

Characterizations: Optical and fluorescence images of the microfluidic device, droplets, and gas-filled capsules were obtained by using a Nikon Eclipse Ti-S fluorescence microscope equipped with a high-speed camera (exposition time 1 μs). The morphologies of nanoparticles were imaged using a Hitachi SU-70 Schottky field emission gun Scanning Electron Microscope (FEG-SEM) and a JEOL FEG Transmission Electron Microscope (FEG-TEM). Samples for SEM were prepared by casting a layer of the GFCs on silicon wafers, and dried at room temperature. TEM samples were prepared from the casting on 300 mesh copper grids covered with carbon film, and dried at room temperature.

Fabrication of microfluidic devices: Monodisperse emulsion droplets were prepared through a co-flow microcapillary device.[21, 30, 31] Briefly, one round glass capillary (World Precision Instruments) with outer and inner diameters of 1.0 mm and 580 μm, respectively, was firstly tapered to achieve an orifice of ~ 40-80 μm by using a micropipette puller (Narishige PC-10) and a microforge (Narishige MF-900), as is shown in Figure SI1. The tapered round capillary was used for the injection of inner fluid. The tapered round capillary and another non-tapered round capillary (as a collection tube) were then assembled into the square capillary with an inner dimension of 1.0 mm. The tip of the tapered round capillary was inserted into the collection tube and both tubes should keep a suitable distance to make the external oil phase flow in the collection tube. Subsequently, a transparent epoxy resin was used to seal the tubes where needed. To ensure the stable generation of monodisperse emulsion droplets, the collection tube is treated with TPFS to render hydrophobic surface property.

Synthesis of gold nanorods: AuNRs were synthesized according to a previously reported literature with some modifications[32-34]. The synthesis can be separated into two steps, the seeding process and the growing process. In brief, the seeds were prepared by injecting 600 μL of 0.01M

$NaBH_4$ into a 10 mL solution of 0.1 M CTAB and 2.5×10^{-4} M $HAuCl_4$ under rapid stirring, followed by keeping in a 30 ºC water bath for ~ 30 min before use. The growing step is described as following. 4.20 g of CTAB and 0.7404 g of sodium oleate were dissolved in 150 mL water (solution 1) in a 500 mL Erlenmeyer flask under heating. After solution 1 was cooled down to room temperature, it was set in a water bath of 30 ºC while adding 10.8 mL of 3 mM $AgNO_3$ solution. 15 minutes later, another 150 mL aqueous solution containing 0.0591 g $HAuCl_4$ was quickly added to solution 1 with stirring at 700 rpm. After 90 minutes, 950 µL HCl (37%) was injected into the solution under stirring at 400 rpm. Wait for another 15 minutes, 240 µL seed solution and 750 µL of 0.064 M ascorbic acid were added to the solution. The solution was taken off the stir-plate and placed in a 30 ºC water bath overnight. The product was purified and concentrated by two cycles of centrifugation with 5000 rpm for future use.

Synthesis of Fe_3O_4: Fe_3O_4 nanoparticles were synthesized according to the previous reports with few modifications.[35, 36] Briefly, 0.994 g $FeCl_2\cdot4H_2O$ and 5.406 g $FeCl_3\cdot6H_2O$ were dissolved in a flask with 500 mL H_2O. Then the above solution was set in a water bath of 30 ºC. 6 mL of 28 % (wt %) $NH_3\cdot H_2O$ was added into the solution with strong stirring. After the color of the solution changed from yellow to dark brown, the reaction was kept on for 25 min more. Then, the sample was washed several times using pure water until the pH value is 7.0. The product was redispersed in water for future use.

RESULTS AND DISCUSSION

Generation of gas-filled capsules (GFCs)

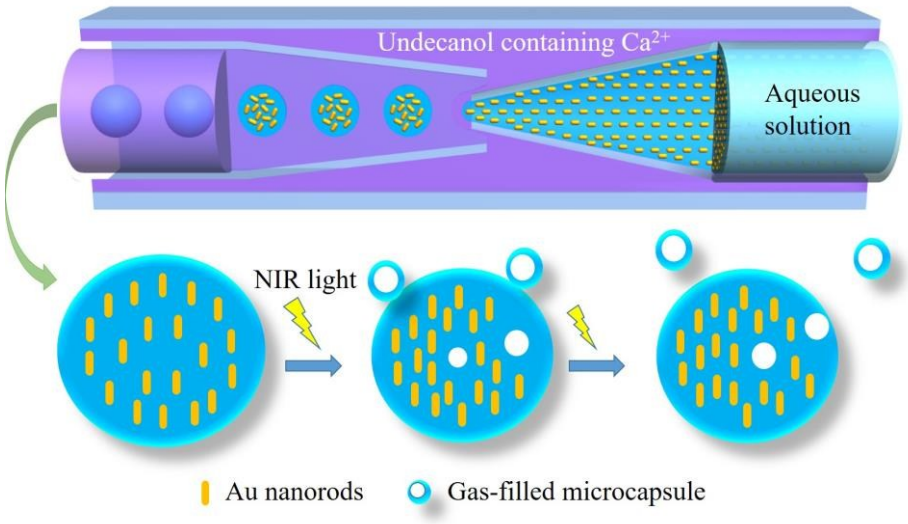

Scheme 1. The microfluidic generation of monodisperse droplets containing AuNRs, alginate and NH_4HCO_3 (top) and NIR-light triggered preparation of GFCs as a result of photothermal effect of AuNRs (bottom).

The fabrication of GFCs involves the generation of AB-containing microcapsules in microfluidics and subsequent light-triggered formation of GFCs with polymer shells (Scheme 1). Monodisperse aqueous droplets were first generated continuously in a single-emulsion microfluidic device. An aqueous solution containing PVA, AuNRs (~0.5 mg/mL), saturated AB and sodium alginate was used as the dispersed phase. A solution of calcium ions (CaI_2) in undecanol was used as the continuous phase. When the two immiscible fluids were forced through a microfluidic capillary, monodisperse droplets were produced due to the interfacial tension and strong shearing force of external flow (Figure 1a). The diffusion of calcium ions from oil to droplet phase crosslinked alginate polymers to generate microcapsules[37], when the droplets were flowing in the downstream channel (Figure 1b). The microcapsules were subsequently transferred and stored in oil (e.g., undecanol, soybean oil) without calcium ions. The size of the microcapsules was controlled in the range of 300 to 1000 µm by tuning the flow rates of fluids, (Figure SI3). The shell thickness of the capsules can be controlled by varying the concentration of calcium ions and the residence time of the droplets in the solution with crosslinker. The microcapsules containing AuNRs and AB are very stable and can be stored for months at room temperature.

AuNRs are known to exhibit strong photothermal effect, that is, the conversion of light to heat.[38, 39] In this work, AuNRs with an aspect ratio of ~4.0 (21.3 ± 2.4 nm in diameter and 80.2 ± 3.7 nm in length) were used to trigger the thermal decomposition of encapsulated AB (Figure SI2a). UV-visible spectrum of the AuNRs shows a strong absorption peak centered at ~800 nm and a weak absorption peak located at ~520 nm corresponding to the longitudinal and transverse mode of plasmonic bands of AuNRs, respectively (Figure SI2b). To initiate the GFC generation, microcapsules containing AuNRs and saturated AB were dispersed in a solution of calcium ions in undecanol (or water). The generation of GFCs from microcapsules was triggered by NIR light with a wavelength of 808 nm (power of 1 ~ 6 W/cm^2 and exposure time < 100 s). Upon the irradiation of NIR light, AB decomposes to release gases, following the reaction equation:

$$(NH_4)HCO_3 \rightarrow CO_2 \uparrow + NH_3 \uparrow + H_2O$$

The gas bubbles kept growing within the aqueous phase of the microcapsules when heat was continuously produced internally from the microcapsules. At certain stage, they emerged out and attached on the surface of the microcapsule (shown in Figure 1c). The relatively small bubbles gradually grew and tend to merge into big bubbles. When the bubbles reached a threshold of diameter, they detached from their mother body of microcapsules (Figure 1d, also see video in supporting information). It is surprising that the surface of the bubbles is coated with a thin layer of alginate polymers. This is confirmed by the following facts: i) The GFCs can be successfully transferred to water phase (Figure 1e, f and Figure SI4) and maintained their dimensions for days, while it is known that both CO_2 and NH_3 bubbles will rapidly dissolve in water; ii) The GFCs burst and collapse upon mechanical punch, and imaging of the residual indicates that there was a film on the surface of water (Figure 1g and Figure SI5a). We presume that the continuous production of gas causes the increase in the internal pressure, forcing gas to be emulsified through pores of crosslinked networks of alginate in the capsule membrane. The crosslinking of the thin layer of alginate solution on the surface of gas bubbles led to the formation of stable GFCs.

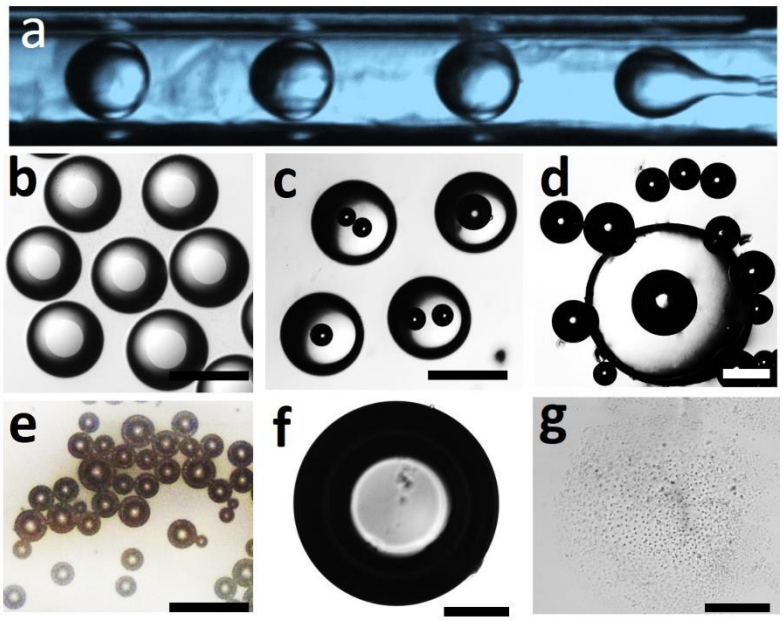

Figure 1. (a-f) Optical microscope images of the formation of droplets in the microchannel (a), products of microdroplets in undecanol (b), bubbles attached to the microcapsules at the initial stage of laser exposure in undecanol (c), bubbles attached to and separated from the microcapsule after laser exposure in undecanol (d), collected GFCs in water (e), a single GFC in water (f). (g) Scanning electron microscope (SEM) image of a broken GFC. Scale bars are 400 μm in (b) and (c), 100 μm in (d) and (e), 25 μm in (f) and (g).

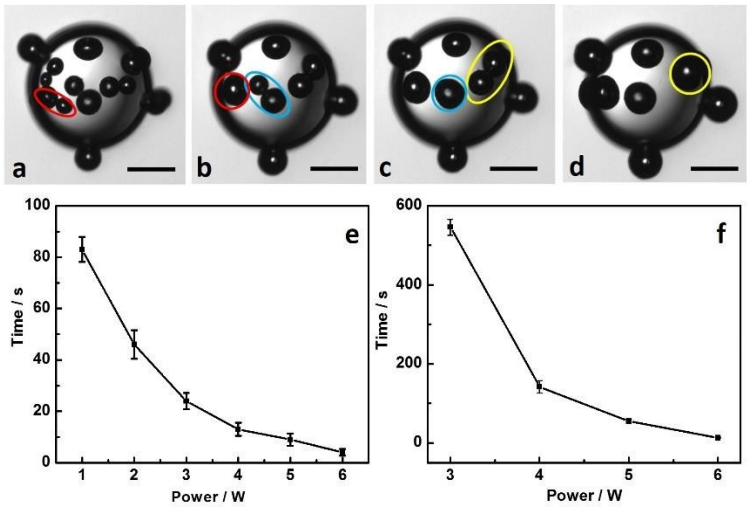

Figure 2. (a-d) Optical microscope images of the merging process of bubbles on the surface of microcapsules upon the irradiation of NIR light. (e) The onset time required for producing

bubbles as a function of laser power. (f) The time required for producing stable bubble released from the main capsule as a function of laser power. Scale bars in (a-d) are 120 μm.

The formation of stable GFCs involves a dynamic emerging of small unstable bubbles (Figure 2a-d). At the initial stage, the membrane of small bubbles was not stable enough, probably due to the short crosslinking time. Hence, the small bubbles tend to merge into bigger ones when they are still exposed to laser, until they reach stable status. It is noted that the membrane of the GFCs is stable enough to avoid them from merging after they are released from the mother body.

We further investigated the kinetics of the NIR light-triggered generation of GFCs by monitoring the onset time for producing the first bubbles. Figure 2e shows that the onset time required for producing bubbles decreases with the increase in the power of NIR laser. This can be explained by the faster decomposition of AB at a higher temperature resulted from more rapid conversion of light to heat. For instance, the time for the first bubble emergence was about 84s with the laser power of 1 W but decreased down to less than 10 s with the laser power of 6W. Similarly, the time required for producing and releasing a stable bubble from the main capsule also decreased with the increase of laser power (Figure 2f). At low power (~1 W), the bubbles cannot be released from the main capsule, largely due to the low internal pressure to force gas through small pores of crosslinked alginate networks. At the power of ~3 W, the first bubble can be released from the main capsule at around 545s, while the release time decreases down to about 58s at a power of 5W.

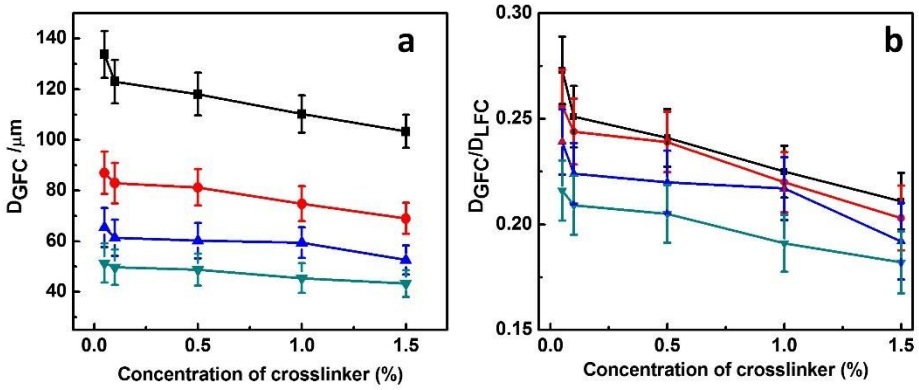

Figure 3. (a) The diameter of GFCs (D_{GFC}) and (b) the diameter ratio of GFCs to mother capsules (D_{GFC}/D_{LFC}) as a function of the concentration of crosslinker (Ca^{2+}) during the formation of microcapsules. The curves in (a) and (b) correspond to initial droplets with a diameter of 492.3, 338.7, 243.9, and 237.6 μm (from top to bottom).

The diameter of GFCs (D_{GFC}) is strongly dependent on the diameter of liquid-filled microcapsule (D_{LFC}) and thickness of capsule membranes which is determined by the concentration of calcium ions (crosslinker) in undecanol. Figure 3a shows that D_{GFC} decreases with the increase in the concentration of crosslinker. This can be explained by the fact that gas bubbles become difficult to be escaped from the capsule membrane — which is thick and has high crosslinking density — of the mother body. Similarly, the diameter ratio of GFCs to mother capsules (D_{GFC}/D_{LFC}) decreased with the increase in crosslinker concentration (Figure 3b). We presume that the pores of the crosslinked alginate networks in the capsule membranes serve as channels for the emulsification of the gases. The higher the crosslinking density of the membrane of main capsules is, the smaller the gas bubbles will be generated from the main body.

Generation of multifunctional GFCs

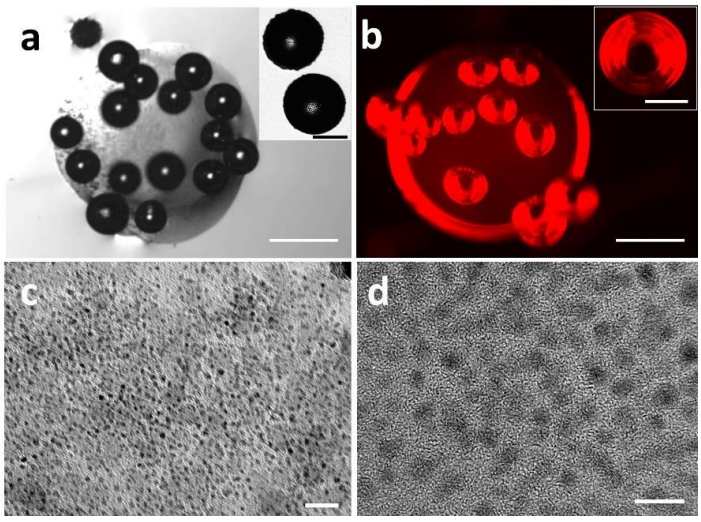

Figure 4. (a,b) Optical and fluorescence microscope image of functional GFCs loaded with iron oxide (a) and QDs (b) in the membrane of the capsules. Insets are high magnification images of functional GFCs. (c,d) TEM images of GFC membrane embedded with iron oxide (c) and QDs (d). Scale bars are 120 μm in (a, b), 100 nm in (c), 50 nm in (d), and 40 μm in inset images.

To demonstrate the multifunctionality of GFCs, various functional substances such as Rhodamine B (RhB), CdSe/ZnS QDs (with a diameter of 20.3 ± 3.1 nm, λ_{em} = 590 nm, λ_{ab} ranging from 450 to 570 nm), and Fe_3O_4 magnetic NPs (with a diameter of 17.5± 2.7 nm), have been introduced into the GFCs. When both iron oxide NPs and AuNRs were encapsulated in the aqueous core of the microcapsules, the irradiation of the capsules with NIR laser led to the generation of GFCs functionalized with iron oxide NPs in the shell (Figure 4a). The iron oxide NPs can be clearly observed in the membrane of GFCs under transmission electron microscopy (TEM) (Figure 4c). The presence of iron oxide particles was also confirmed by the directional motion of GFCs under magnetic field (Figure SI7,8). It is interesting that no AuNRs can be found in the membrane of GFCs under TEM. We presume that AuNRs (~21.3 nm in diameter and 80.2 nm in length) are too large to be forced through alginate networks of the capsule membrane. QDs can also be embedded into the shell of gas bubbles using the same method, as indicated by the fluorescence emission of the GFCs under fluorescence microscope (Figure 4b and Figure SI9). The clear crystalline structures of QDs in Figure 4d further confirmed the loading of quantum dots in the membrane. Moreover, Dyes and drug-model molecules can also be embedded inside the GFC membranes (Figure SI10), which may provide another perspective for drug delivery.

Pressure response of GFCs

We further demonstrated the use of the GFCs as a pressure sensor based on the compressibility of the GFCs (Figure 5a-a′). The ideal gas law indicates $pV=nRT$, where, p is the outside pressure, V is the volume of gas, n is the molar value, R is the Boltzmann constant, and T is the temperature. A relationship between p and r (the diameter of bubbles) can be deduced as $r \propto p^{-1/3}$. Figure 5c shows that the diameter of GFC decreases from 163.7 μm to 95.1 μm with the increase of applied pressure in the range of 0.1 to 0.55 kPa, following the abovementioned equation. This GFC sensor is reversible, *i.e.*, when the pressure is removed, the size of the GFC goes back from 95.1 μm to the original size of 163.7 μm. The GF-based pressure sensors may find applications in such as internal pressure sensors of tumors or blood vessels.[40-42]

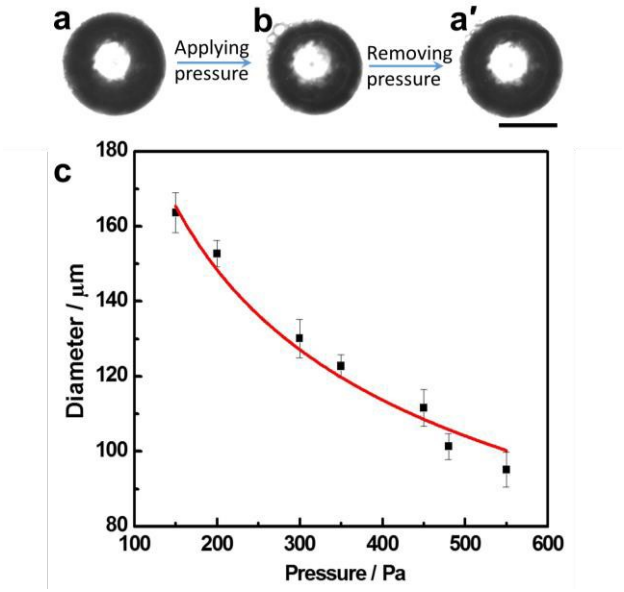

Figure 5. (a-a′) Microscopy images of GFCs at different pressures: 0.150 kPa (a), 0.550 kPa (b), and 0.150 kPa (a′). (c) The diameter of GFCs as a function of surrounding pressure. The plot is fitted with an equation of $r \propto p^{-1/3}$. The scale bar is 100 μm.

Conclusions

We presented a novel strategy for the generation of GFCs on demand by combining continuous microfluidic generation of microcapsules and photothermal triggered chemical reaction. AuNRs were utilized as the heat source to trigger the reaction of gas production, as a result of their photothermal effect upon the irradiation of NIR light. Thermal decomposition of encapsulated ammonium bicarbonate was used to generate CO_2 gases for the formation of GFCs. The resulting CO2 bubbles are coated with a thin membrane of crosslinked alginate. The GFCs can be readily functionalized with inorganic NPs in the alginate membranes. The functional GFCs may find applications in such as bioimaging, drug delivery, and sensors.

Acknowledgements

Z.N. gratefully acknowledges the financial support from the American Chemical Society Petroleum Research Fund (PRF no. 53461-DNI7), National Science Foundation CAREER award (DMR-1255377), National Science Foundation (CHE-1505839), and 3M Non-tenured Faculty Award. K.S. is grateful for the financial support from National Natural Science Foundation of

China (no. 21273059, 21003032). We also thank the Maryland NanoCenter and its NispLab for SEM/TEM imaging. The NispLab is supported in part by the NSF as a MRSEC Shared Experimental Facilities. L. W thanks for the short-term visiting program of Harbin Institute of Technology.

References

1. E. Stride and M. Edirisinghe, *Soft matter*, 2008, **4**, 2350-2359.
2. K. Pancholi, U. Farook, R. Moaleji, E. Stride and M. Edirisinghe, *European Biophysics Journal*, 2008, **37**, 515-520.
3. S. A. Peyman, R. H. Abou-Saleh, J. R. McLaughlan, N. Ingram, B. R. Johnson, K. Critchley, S. Freear, J. A. Evans, A. F. Markham and P. L. Coletta, *Lab on a Chip*, 2012, **12**, 4544-4552.
4. G. R. Heath, R. H. Abou-Saleh, S. A. Peyman, B. R. Johnson, S. D. Connell and S. D. Evans, *Soft matter*, 2014, **10**, 694-700.
5. F. Xie, J. M. Tsutsui, J. Lof, E. C. Unger, J. Johanning, W. C. Culp, T. Matsunaga and T. R. Porter, *Ultrasound in medicine & biology*, 2005, **31**, 979-985.
6. R. Villa, B. Cerroni, L. Viganò, S. Margheritelli, G. Abolafio, L. Oddo, G. Paradossi and N. Zaffaroni, *Colloids and Surfaces B: Biointerfaces*, 2013, **110**, 434-442.
7. F. S. Foster, P. N. Burns, D. H. Simpson, S. R. Wilson, D. A. Christopher and D. E. Goertz, *Cancer and Metastasis reviews*, 2000, **19**, 131-138.
8. F. S. Foster, C. J. Pavlin, K. A. Harasiewicz, D. A. Christopher and D. H. Turnbull, *Ultrasound in Medicine & Biology*, 2000, **26**, 1-27.
9. X. Zhao, X. Zhang, L. Xue, J. Wang, B. Shen, C. Luo and Q. Wang, *Colloids and Surfaces A: Physicochemical and Engineering Aspects*, 2014, **452**, 59-64.
10. J. I. Park, D. Jagadeesan, R. Williams, W. Oakden, S. Chung, G. J. Stanisz and E. Kumacheva, *Acs Nano*, 2010, **4**, 6579-6586.
11. K. Ferrara, R. Pollard and M. Borden, *Biomedical Engineering*, 2007, **9**.
12. H. Ke, Z. Xing, B. Zhao, J. Wang, J. Liu, C. Guo, X. Yue, S. Liu, Z. Tang and Z. Dai, *Nanotechnology*, 2009, **20**, 425105.
13. F. Yang, Y. Li, Z. Chen, Y. Zhang, J. Wu and N. Gu, *Biomaterials*, 2009, **30**, 3882-3890.
14. K.-J. Chen, H.-F. Liang, H.-L. Chen, Y. Wang, P.-Y. Cheng, H.-L. Liu, Y. Xia and H.-W. Sung, *ACS nano*, **2013,** 7, (1), 438-446.
15. F. Cavalieri, M. Zhou, F. Caruso and M. Ashokkumar, *Chemical Communications*, 2011, **47**, 4096-4098.
16. F. Cavalieri, M. Ashokkumar, F. Grieser and F. Caruso, *Langmuir*, 2008, **24**, 10078-10083.
17. K. Bjerknes, K. Dyrstad, G. Smistad and I. Agerkvist, *Drug development and industrial pharmacy*, 2000, **26**, 847-856.
18. M. R. Böhmer, R. Schroeders, J. A. Steenbakkers, S. H. de Winter, P. A. Duineveld, J. Lub, W. P. Nijssen, J. A. Pikkemaat and H. R. Stapert, *Colloids and Surfaces A: Physicochemical and Engineering Aspects*, 2006, **289**, 96-104.
19. M. H. Lee, V. Prasad and D. Lee, *Langmuir*, 2009, **26**, 2227-2230.
20. A. Abbaspourrad, W. J. Duncanson, N. Lebedeva, S.-H. Kim, A. P. Zhushma, S. S. Datta, P. A. Dayton, S. S. Sheiko, M. Rubinstein and D. A. Weitz, *Langmuir*, 2013, **29**, 12352-12357.
21. W. J. Duncanson, A. Abbaspourrad, H. C. Shum, S.-H. Kim, L. L. Adams and D. A. Weitz, *Langmuir*, 2012, **28**, 6742-6745.
22. M. Seo, I. Gorelikov, R. Williams and N. Matsuura, *Langmuir*, 2010, **26**, 13855-13860.
23. M. H. Lee and D. Lee, *Soft Matter*, 2010, **6**, 4326-4330.
24. S. Sirsi and M. Borden, *Bubble Science, Engineering & Technology*, 2009, **1**, 3-17.
25. M. A. Borden and M. L. Longo, *Langmuir*, 2002, **18**, 9225-9233.
26. M. W. Keller, S. S. Segal, S. Kaul and B. Duling, *Circulation research*, 1989, **65**, 458-467.
27. S. Otis, M. Rush and R. Boyajian, *Stroke*, 1995, **26**, 203-209.
28. D. Taeymans, A. Andersson, P. Ashby, I. Blank, P. Gondé, P. v. Eijck, V. Faivre, S. P. Lalljie, H. Lingnert and M. Lindblom, *Journal of AOAC International*, 2005, **88**, 234-241.
29. B. G. Osborne, T. Fearn, A. R. Miller and S. Douglas, *Journal of the Science of Food and Agriculture*, 1984, **35**, 99-105.

30. Z. Nie, J. I. Park, W. Li, S. A. Bon and E. Kumacheva, *Journal of the American Chemical Society*, 2008, **130**, 16508-16509.
31. L. R. Arriaga, S. S. Datta, S.-H. Kim, E. Amstad, T. E. Kodger, F. Monroy and D. A. Weitz, *Small*, 2014, **10**, 950-956.
32. J. He, Z. Wei, L. Wang, Z. Tomova, T. Babu, C. Wang, X. Han, J. T. Fourkas and Z. Nie, *Angewandte Chemie*, 2013, **125**, 2523-2528.
33. X. Ye, C. Zheng, J. Chen, Y. Gao and C. B. Murray, *Nano letters*, 2013, **13**, 765-771.
34. L. Wang, Y. Liu, J. He, M. J. Hourwitz, Y. Yang, J. T. Fourkas, X. Han and Z. Nie, *Small*, 2015, **11**, 3762-3767.
35. P. Tserotas, T. Lazaridis and E. Statharas, *Key Engineering Materials*, 2014, **605**, 689-692.
36. P. Xu, G. Zeng, D. Huang, S. Hu, C. Feng, C. Lai, M. Zhao, C. Huang, N. Li and Z. Wei, *Colloids and Surfaces A: Physicochemical and Engineering Aspects*, 2013, **419**, 147-155.
37. H. Zhang, E. Tumarkin, R. Peerani, Z. Nie, R. M. A. Sullan, G. C. Walker and E. Kumacheva, *Journal of the American Chemical Society*, 2006, **128**, 12205-12210.
38. A. M. Alkilany, L. B. Thompson, S. P. Boulos, P. N. Sisco and C. J. Murphy, *Advanced drug delivery reviews*, 2012, **64**, 190-199.
39. S. Link, C. Burda, M. Mohamed, B. Nikoobakht and M. El-Sayed, *The Journal of Physical Chemistry A*, 1999, **103**, 1165-1170.
40. V. Thamilselvan and M. D. Basson, *Gastroenterology*, 2004, **126**, 8-18.
41. M. D. Basson, C. F. Yu, O. Herden-Kirchoff, M. Ellermeier, M. A. Sanders, R. C. Merrell and B. E. Sumpio, *Journal of cellular biochemistry*, 2000, **78**, 47-61.
42. V. Thamilselvan, D. H. Craig and M. D. Basson, *The FASEB Journal*, 2007, **21**, 1730-1741.

Graphical Abstract:

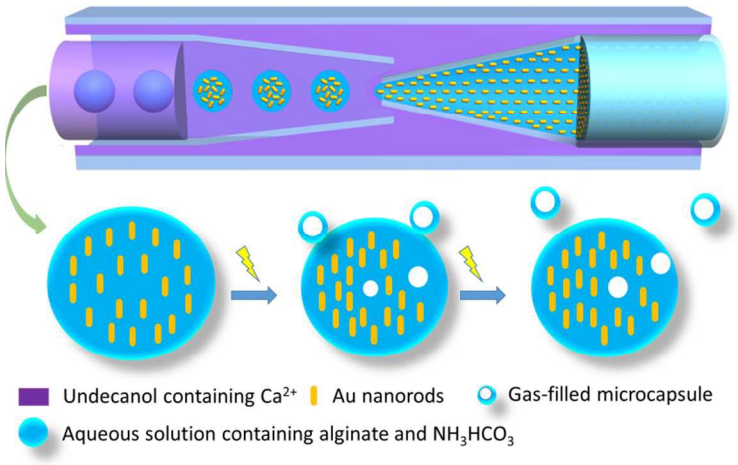

This Communication describes a novel strategy for the generation of gas-filled capsules (GFCs) on demand by combining microfluidic generation of microcapsules and photothermal triggered thermal decomposition of ammonium bicarbonate. The functional GFCs with inorganic nanoparticles in the membrane may find applications in bioimaging, drug delivery, and pressure sensors.